HHS Public Access

Author manuscript

Mol Pharm. Author manuscript; available in PMC 2017 March 01.

Published in final edited form as:

Mol Pharm. 2016 June 06; 13(6): 2070–2083. doi:10.1021/acs.molpharmaceut.6b00205.

Mechanistic Nanotherapeutic Approach Based on siRNA-Mediated DJ-1 Protein Suppression for Platinum-Resistant Ovarian Cancer

Canan Schumann[1], **Stephanie Chan**[1], **Oleh Khalimonchuk**[2,3,4], **Shannon Khal**[1], **Vitaliya Moskal**[1], **Vidhi Shah**[1], **Adam W. G. Alani**[1], **Olena Taratula**[1,*], and **Oleh Taratula**[1,*]

[1]Department of Pharmaceutical Sciences, College of Pharmacy, Oregon State University, Portland, OR 97201, USA

[2]Department of Biochemistry, University of Nebraska-Lincoln, Lincoln, NE 68588, USA

[3]Nebraska Redox Biology Center, University of Nebraska-Lincoln, Lincoln, NE 68588, USA

[4]Fred & Pamela Buffett Cancer Center, University of Nebraska Medical Center, Omaha NE, 68198, USA

Abstract

We report an efficient therapeutic modality for platinum resistant ovarian cancer based on siRNA-mediated suppression of a multifunctional DJ-1 protein that is responsible for the proliferation, growth, invasion, oxidative stress and overall survival of various cancers. The developed therapeutic strategy can work alone or in concert with a low dose of the first line chemotherapeutic agent cisplatin, to elicit a maximal therapeutic response. To achieve an efficient DJ-1 knockdown, we constructed the polypropylenimine dendrimer-based nanoplatform targeted to LHRH receptors overexpressed on ovarian cancer cells. The quantitative PCR and western immunoblotting analysis, revealed that the delivered *DJ-1* siRNA downregulated the expression of targeted mRNA and corresponding protein by more than 80% in various ovarian cancer cells. It was further demonstrated that siRNA-mediated DJ-1 suppression dramatically impaired proliferation, viability and migration of the employed ovarian cancer cells. Finally, the combinatorial approach led to the most pronounced therapeutic response in all the studied cell lines, outperforming both siRNA-mediated DJ-1 knockdown and cisplatin treatment alone. It is noteworthy that the platinum-resistant cancer cells (A2780/CDDP) with the highest basal level of DJ-1 protein are most susceptible to the developed therapy and this susceptibility declines with decreasing basal levels of DJ-1. Finally, we interrogate the molecular underpinnings of the DJ-1 knockdown effects in the

*Corresponding author. Tel.: +503-346-4704, Fax.: +503-494-8797, Oleh.Taratula@oregonstate.edu, Olena.Taratula@oregonstate.edu, Department of Pharmaceutical Sciences, College of Pharmacy, Collaborative Life Science Building, 2730 SW Moody Ave., Mail Code: CL5CP, Portland, OR 97201-5042.

The authors declare no competing financial interest.

Supporting Information

Representative IC_{50} curves for CDDP in A2780/CDDP, ES2 and IGROV1 ovarian cancer cells, real time proliferation curves of A2780 ovarian cancer cells, qPCR data for A2780/CDDP, ES2 and IGROV1 cells treated with the nanoplatform containing scrambled siRNA, flow cytometry histogram of SKOV3 cells treated with the constructed nanoplatform, qPCR data for A2780/CDDP, ES2 and IGROV1 cells treated with the nanoplatform containing 0.25, 0.5, and 1.0 μM *DJ-1* siRNA, fluorescence microscopy images demonstrating expression of DJ-1 protein in tumor tissues, and fluorescence microscopy images demonstrating caspase-3/7 activity (green fluorescence) in A2780/CDDP, ES2 and IGROV1 cells

treatment of the ovarian cancer cells. By using various experimental techniques, it was revealed that DJ-1 depletion: (1) decreases the activity of the Akt pathway, thereby reducing cellular proliferation, migration and increasing the antiproliferative effect of cisplatin on ovarian cancer cells; (2) enhances the activity of p53 tumor suppressor protein therefore restoring cell cycle arrest functionality and upregulating the Bax-caspase pathway, triggering cell death; and (3) weakens the cellular defense mechanisms against inherited oxidative stress thereby increasing toxic intracellular radicals and amplifying the reactive oxygen species created by the administration of cisplatin.

Graphical Abstract

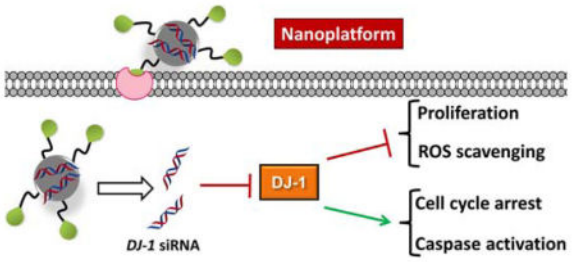

Keywords

DJ-1; ovarian cancer; siRNA; LHRH; dendrimer; nanomedicine; cisplatin

INTRODUCTION

Ovarian cancer kills over 14,000 women every year in the United States alone and is known as the “silent killer” due to the fact that very few symptoms are present until the later stages of the disease’s development.[1] Treatment options for advanced stage ovarian cancer are limited and consist primarily of maximal debulking surgery followed by chemotherapy.[2] The main problem of cytoreductive surgery is related to the fact that it cannot provide complete cancer resection and the need to administer chemotherapy post-surgery is of the utmost importance to reduce ovarian cancer recurrence.[3, 4] A combined chemotherapy regimen, which involves two or more chemotherapeutic drugs such as platinum- or taxane-based agents, has been shown to be most beneficial when treating ovarian cancer, as it targets multiple cancer progression pathways.[5, 6] The efficacy of conventional chemotherapy, however, is limited by the aggressive nature of the ovarian cancer cells as well as their ability to upregulate specific proteins responsible for multidrug resistance.[7] Moreover, a drawback of the current combinatorial chemotherapy is an increase of systemic side effects when several drugs are added to the regimen.[6] The adverse side effects in healthy organs invariably impose dose reduction of chemotherapeutic drugs or even discontinuance of therapy. Hence, there is a need to develop a novel therapeutic approach that can work alone or in concert with a low dose of a single chemotherapeutic drug to elicit a maximal therapeutic response while minimizing the risk of physically detrimental side effects.

Recently DJ-1, also known as PARK7, has been identified as an oncogenic driver and a significant amount of experimental evidences has indicated that it is frequently

overexpressed in various human cancers, including prostate cancer, non-small cell lung carcinoma, pancreatic ductal adenocarcinoma, and ovarian carcinoma.[8, 9] It has been also demonstrated that higher DJ-1 expression is positively associated with decreased survival in patients with various tumor types including non-small cell lung cancer, esophageal squamous cell carcinoma and ovarian cancer.[10–12] DJ-1 is a multifaceted protein and to date it has been found to be responsible for the proliferation, growth, invasion, and overall survival of various cancers.[9] DJ-1 is known to affect several cellular processes that drive cancer progression (Figure 1). These processes include: (1) *Proliferation,* where DJ-1 inhibits the actions of phosphatase and tensin homolog (PTEN) allowing the Akt proliferation pathway to proceed forward unchecked (Figure 1A);[9, 13, 14] (2) *Apoptosis* and *cell cycle arrest,* wherein DJ-1 binds to tumor protein p53 and inhibits its translocation to the nucleus, thereby preventing enhanced expression of various anti-apoptotic proteins, as well as p53's ability to arrest cell cycle progression (Figure 1B);[9, 15] (3) *Oxidative stress responses*, DJ-1 can directly scavenge reactive oxygen species (ROS), as well as enhance synthesis of reduced glutathione (GSH), and influence the destabilization of the NRF2/Keap1 complex, thus allowing transcriptional factor NRF2 to accumulate in the nucleus, and upregulate expression of multiple antioxidant proteins (Figure 1C). [16, 17] Additionally, DJ-1 has been identified as a cisplatin (CDDP) resistant biomarker in both non-small cell lung cancer and pancreatic cancer, making DJ-1 a potentially important therapeutic target for the treatment of DJ-1 overexpressing platinum resistant ovarian cancer.[1812] Finally, several studies reported that an increase in cytosolic DJ-1 is negatively correlated with overall ovarian cancer cell survival.[9, 10]

Based on the aforementioned facts, it has been hypothesized that siRNA-mediated silencing of DJ-1 protein in combination with CDDP as a first line chemotherapeutic agent, [19] can result in enhanced therapeutic efficacy for ovarian cancer while minimizing adverse side effects. To verify the proposed hypothesis and achieve an efficient and targeted delivery of *DJ-1* siRNA to various ovarian cancer cells, we constructed a nanoparticle-based siRNA delivery system, which contains four components (Figure 2): (1) siRNA molecules to attenuate *DJ-1* gene expression; (2) Polypropylenimine (PPI) dendrimer to act as a siRNA carrier; (3) polyethylene glycol (PEG) to enhance stability and biocompatibility of the nanoplatform; and (4) LHRH peptide, serving as a specific targeting moiety to ovarian cancer cells.[20] By incorporating the prepared siRNA nanoplatform (siRNA-NP) and the first line chemotherapeutic agent CDDP, we have developed an efficient combinatorial therapeutic approach for the treatment of platinum-resistant ovarian cancer cells and elucidate the underlying role of the DJ-1 protein in ovarian cancer cells survival and growth. Herein, we provide evidence for the abrogation of the platinum resistant phenotype of several ovarian cancer cell lines via the suppression of DJ-1 protein. Our report relies on three major observations: DJ-1 depletion (1) decreases the activity of the Akt pathway, thereby reducing cellular proliferation, migration, and increasing the antiproliferative effect of CDDP on ovarian cancer cells; (2) enhances the activity of p53 tumor suppressor protein therefore restoring cell cycle arrest functionality and upregulating the Bax-caspase pathway, triggering cell death; (3) weakens cellular ROS defense mechanisms thereby increasing toxic intracellular radicals and amplifying the ROS created by the administration of CDDP.

MATERIALS AND METHODS

Materials

Human ovarian carcinoma A2780/CDDP, ES2, IGROV1 and SKOV3 cell lines were purchased form ATCC (Manassas, VA). Generation 4 poly(propylene imine) dendrimer (PPIG4) was obtained from SyMO-Chem (The Netherlands). Luteinizing Hormone Releasing Hormone (LHRH) peptide (Gln-His-Trp-Ser-Tyr-DLys(DCys)-Leu-Arg-Pro-NH-Et) was purchased from Amersham Peptide Co. (Sunnyvale, CA). α-Maleimide-ω-N-hydroxysuccinimide ester poly(ethylene glycol) (MAL-PEG-NHS 5 kDa) was acquired from NOF Corporation (White Plains, NY). 2,4,6-Trinitrobenzene Sulfonic Acid (TNBS) assay was purchased from Thermo Scientific (Waltham, MA). *DJ-1* Stealth siRNA and Vybrant Dye Cycle Green were purchased from Life Technologies (Grand Island, NY). siGLO Red Transfection Indicator was obtained from GE Dharmacon (Lafayette, CO). Roswell Park Memorial Institute (RPMI) media and Dulbecco's Phosphate Buffered Saline (DPBS) were acquired from Mediatech (Manassas, VA). Calcein AM cell viability assay and GSH-Glo assay kits were purchased from Enzo Life Sciences (Farmingdale, NY). 10% pre-cast Tris-Glycine acrylamide gels and Trans-Blot Turbo packs were obtained from Bio-Rad (Hercules, CA). Peroxy Yellow 1 (PY1) was purchased from Sigma-Aldrich (St. Louis, MO). All other chemicals and supplies were obtained through VWR International (Radnor, PA).

Methods

Synthesis and characterization of the nanoplatform for siRNA delivery—PPIG4 dendrimer-based nanoplatform loaded with siRNA (siRNA-NP) was constructed according to the previously described procedure.[21–23] Synthesis of the siRNA-NP was initiated by mixing *DJ-1* siRNA (10 μM) with the PPIG4 at a nitrogen to phosphate (N/P) ratio of 4 in MilliQ water and vortexing the reaction mixture for 1 h at room temperature. Afterwards, MAL-PEG-NHS was added to the reaction mixture (NHS : NH_2 = 1 : 5 molar ratio) and the solution was vortexed during 1 h at room temperature. Finally, the LHRH peptide was introduced to the solution (MAL-PEG-NHS : LHRH = 1 : 5 molar ratio) and the reaction mixture was incubated for 12 h at room temperature. The complexation efficiency of siRNA with PPIG4 was validated via gel retardation assay as previously described.[22–26] Surface modification of siRNA-PPIG4 complexes with PEG and LHRH peptide was confirmed by using TNBS and the bicinchoninic acid assay (BCA) assays according to the previously reported procedures.[23, 27] The hydrodynamic diameter and zeta potential of the developed nanoplatform were evaluated by employing dynamic light scattering (Malvern ZetaSizer NanoSeries, Malvern, U.K.) as previously described.[28]

Cell Culture—A2780/CDDP, ES2, IGROV1, SKOV3 human ovarian carcinoma cells were cultured using RPMI culture media supplemented with 10% FBS and 1% streptomycin/ampicillin. Cells were grown at 37 °C in a humidified atmosphere of 5% CO_2 (v/v) in air.[28–30]

Cellular internalization of the siRNA-NP—Flow cytometry was employed to evaluate cellular internalization efficiency of the siRNA-NP.[27, 29] Briefly all cells were seeded in a

six well cell culture plate at a density of 3×10^5 cells per well in RPMI media and allowed to adhere to the plate overnight. Then, the prepared nanoplatform loaded with Dy-547 labeled siRNA, was added to the cells (siRNA = 1 μM) and incubated for 24 h prior to flow cytometry analysis. The cells were trypsinized, collected in 0.5 mL Eppendorf tubes, washed 3 times with DPBS, resuspended in 200 μL DPBS, and analyzed using an Accuri C6 flow cytometer (BD Biosciences, San Jose, CA). All data analyses were performed using the BD C6 Accuri software. For the quantification of siRNA internalization via flow cytometry no gating was used. Before the cellular uptake analysis non-treated cells were evaluated and the auto fluorescence was measured and recorded to be in the 10^3 fluorescence decade for all the tested cell lines. Then the cells treated with the constructed nanoplatform were analyzed and histograms were plotted. To determine the percentage of cells transfected with the dye-labeled siRNA we drew a line using the BD software at the 10^3 decade and then allowed the software to calculate percent cells containing fluorescently labeled siRNA.

Calcein AM Cell Viability Assay—For all cell viability endpoint experiments a modified Calcein AM assay was performed by following our previously published protocol.[21, 27, 29–31]

Real Time Quantitative PCR (qPCR) analysis—qPCR was used to validate gene expression in each cell model before and after treatment with the siRNA-NP (siRNA = 1 μM) for 24 h.[21, 22] Briefly, total RNA was extracted from the treated cells using an RNeasy extraction kit (Qiagen, Hilden, Germany) and RNA concentrations were determined using a BioSpec-nano UV-Vis Spectrophotometer (Shimadzu, Columbia, MD). Reverse transcription was carried out using High-Capacity cDNA Reverse Transcription Kit (Thermo Scientific) according to manufacturer's protocol. Following cDNA preparation 100 ng of each sample was loaded into the 96 well qPCR plate at a final volume of 20 μL, using β-actin as endogenous control. Taqman primers for all gene targets were used for cDNA template amplification. The qPCR plate was read using a Applied Biosystems Step One Plus qPCR system (Thermo Scientific) with an initial cycle step at 50°C for 2 min followed by 40 cycles of 95°C for 15 s then 60°C for 1 min. The C_t threshold values were automatically determined by the software, and all samples were done in triplicate for statistical analysis.

Western Immunoblotting analysis—Western immunoblotting analysis was performed to confirm intracellular protein levels in all studied cell lines before and after treatment with the siRNA-NP.[21] Briefly all cell lines were seeded in T-25 flask at a cell density of 20×10^5 and incubated overnight at 37°C. Afterward the media was removed and 3.6 mL of fresh media along with 0.4 mL of *DJ-1* siRNA-NP was added to each flask (total volume 4 mL; final siRNA concentration = 1 μM). The cells were collected and analyzed at various time points. The immunoblotting procedure was carried out via our previously published protocol.[21] The antibodies were purchased from Thermo Scientific (Waltham, MA) and antibody dilutions used in each experiment are as follows: DJ-1 (1:1000), NRF2 (1μg/mL), p53 (1:500), phosphoAkt (1μg/mL), and β-actin (1:5000). The western blot band quantification analysis was performed using ImageJ software. Band intensities of the tested proteins are expressed as the percentage of the β-actin band intensity, which was set to 100%.

ROS and GSH measurements—PY-1 and Glo-GSH Glutathione (Promega, Madison, WI) kit-based assays were employed to evaluate intracellular levels of hydrogen peroxide (H_2O_2) and GSH respectively in all cell lines prior to and after treatment with the siRNA-NP. The PY-1 assay was performed as per our previously published procedure.[21] For GSH measurements, all cells were seeded at a density of 5×10^3 in a clear bottom opaque walled 96 well plate to increase signal intensity. Then the cells were treated with the siRNA-NP (1μM) for 24 h, followed by the assaying procedure according to the manufacture protocol. The luminescence was read and analyzed using a Biotek synergy HT plate reader and software (Biotek, Winooski, VT).

Real time cellular proliferation study—Cellular proliferation was measured using the xCELLigence real time proliferation platform (ACEA Biosciences, San Diego, CA).[21] Prior to the assay, the E-plates were coated with 50 μL of fibronectin (10μg/mL) (Sigma-Aldrich), per manufacturer's protocol, and left in the biosafety cabinet for 30 min. Subsequently, the plates were aspirated and 100 μL of cell free media was added to each well, followed by a 30 min equilibration period in the bio safety cabinet. The plates were then loaded onto the instrument and background measurements were recorded for each of them using the RTCA Software 1.2. Next, cells were seeded in each plate at a cellular that it resulted in growth that did not reach 100% confluency in a 96 h time period density (A2780/CDDP: 5,000 cells/well; ES2: 2,500 cells/well; IGROV1: 5,000 cells/well) and placed back into the incubator to adhere to the plate before analysis. Once the cells adhered to the plate, they were placed onto the proliferation platform and the experiment was started. After 2 h, 10 μL of media was removed from the wells assigned for *DJ-1* siRNA treatment alone and combinatorial therapy. Ten μL of 10 μM *DJ-1* siRNA-NP solution were added to the remaining 90 μL of media in each well, resulting in a total volume of 100 μL and a final *DJ-1* siRNA concentration of 1 μM. Following a 24 h incubation period with the *DJ-1* siRNA-NP, an additional 90 μL of media was added to the wells assigned for CDDP treatment only and combinatorial therapy. Then, 10 μL of the corresponding concentrations of CDDP was added to these wells to achieve the required IC50 concentrations for each cell line (A780/CDDP = 23.6 μM, ES2 = 3.8 μM, and IGROV = 1.9 μM). The IC_{50} concentrations for each cell line were determined by using xCELLigence real time proliferation platform in time dependent manner (Figure S1). In case of the control and *DJ-1* siRNA therapy only, 100 μL of media was added to the corresponding wells. The plates were then monitored for 96 h and analyzed using RTCA Software 1.2.

Migration Assay—Cell migration was evaluated using a modified wound healing assay.[32] Briefly, A2780/CDDP, ES2, and IGROV1 cells were seeded in a 6-well plate at a density of 2.5×10^5 cells per well and allowed to reach ~85% confluency before treatment. Afterwards the scratch was made in a cell monolayer using a 200μL pipette tip. Immediately after the scratching, the cells were washed with DPBS to remove any cellular debris, followed by addition of fresh media containing the nanoplatform loaded with *DJ-1* siRNA (final concentration 1μM) to the respective wells. After 24 h, CDDP was added to the corresponding wells assigned for CDDP alone and combinatorial therapies at the following concentrations (A780/CDDP = 23.6 μM, ES2 = 3.8 μM, and IGROV = 1.9 μM). Images of the cells were taken at 0, 24, and 48 h after a scratch was made to monitor cellular

movement and gap reduction. Wound widths after 0 and 48 h were measured and % wound closure was calculated as follows:

$$\text{Wound closure}\ (\%) = (W_{0h} - W_{48h})/W_{0h} \times 100,$$

where W_{0h} and W_{48h} are the wound widths before and 48 h after treatment.

Cell cycle analysis—All cell lines were seeded in 6 well cell culture plates at a density of 3×10^5 cells per well and allowed to incubate at 37°C in 5% CO_2 overnight. The following day the media was removed and 1.8 mL of media along with 0.2 mL of 10 μM *DJ-1* siRNA loaded in the nanoplatform was added to the wells assigned for *DJ-1* siRNA only and combinatorial therapies, followed by an incubation period of 24 h. After 24 h CDDP was added to the wells assigned for CDDP and combinatorial treatments and incubated for another 24 h. The next day the cells were trypsinized, collected in 1.5 mL Eppendorf tubes, and washed 3 times with DPBS. After washing the cells Vybrant Dye Cycle Green was added to each tube according to the manufacturer's protocol and incubated for 2 h at 37°C in 5% CO_2 before flow cytometry analysis. All data was analyzed using BD C6 Accuri software.

Caspase assay—The caspase assay (Thermo Fisher, Brookfield, WI) was performed to quantify caspase activity in the used cell lines after each treatment. All cell lines were seeded at a density of 5×10^3 cells per well in a black opaque walled clear bottom 96 well plate (Corning, Corning, NY) and incubated overnight at 37°C and 5% CO_2. The following day cells were treated with CDDP, siRNA-NP and combinatorial therapy as described above. After treatment, cells were then labeled with 7.5 μM CellEvent™ Caspase-3/7 Green Detection Reagent for 30 minutes at 37°C and fluorescence was measured using a multi-well plate reader (Synergy HT, BioTek Instruments, Winooski, VT) with 485 nm excitation and 528 nm emission filters. Cells were also imaged with an EVOS FL Cell Imaging System (Life Technologies, Grand Island, NY).

Statistical analysis—Data was analyzed using descriptive statistics, single-factor analysis of variance (ANOVA), and presented as mean values ± standard deviation (SD) from three to six independent measurements. The comparison among groups was performed by the independent sample Student's *t* test. The difference between variants was considered significant at $p < 0.05$.

RESULTS AND DISCUSSION

Selection and Characterization of Ovarian Cancer Models

To evaluate the therapeutic effect of DJ-1 protein suppression alone or in combination with CDDP for ovarian cancer treatment, three characteristically different human ovarian carcinoma cell lines such as A2780/CDDP, ES2 and IGROV-1 of various origins, phenotypes, growths rates and CDDP resistance levels were employed. The A2780/CDDP human epithelial ovarian cancer cell line (doubling time = 25 h) is highly resistant to the CDDP.[33] On the contrary, the ES2 human clear cell adenocarcinoma cell line (doubling time

= 19 h) exhibits low to moderate resistance to a number of chemotherapeutic drugs including CDDP.[33] Finally, the IGROV1 human ovarian carcinoma cell line of the mixed origin (doubling time = 27 h) is sensitive to CDDP.[33, 34] To experimentally confirm the indicated resistibility of the employed cancer cell lines to the CDDP, their real time proliferation profiles, after incubation with various concentrations of the drug, were measured and the IC50 values of 23.6 μM, 3.8 μM and 1.9 μM were obtained for A2780/CDDP, ES2 and IGROV-1, respectively (Figure S1). According to qPCR and immunoblot analyses, all tested ovarian cancer cell lines overexpress DJ-1 when compared to non-malignant HUVEC cells (Figure 3A). The selection and use of HUVEC cells as a control was determined on the basis that HUVEC cells are a non-cancerous cell line and they are of epithelial origin as well as the tested ovarian cancer cells. HUVEC cells were employed as an intracellular base line of the metabolic activities of a normally functioning cell. Moreover, the platinum-resistant A2780/CDDP cells exhibited 1.8- and 2.4-fold increase in the basal level of DJ-1 mRNA as compared to the platinum-sensitive ES2 and IGROV cells, respectively (Figure 3A). The obtained results are in a good agreement with previous reports indicating that higher expression levels of DJ-1 increase the chemoresistance of cancer cells by inhibiting various apoptotic pathways.[9, 18] For example, the proteomic studies performed by Zeng *et al.* demonstrated that CDDP resistant lung cancer cells exhibited a 5.4-fold increase in basal level of DJ-1 relative to their drug-sensitive counterparts.[12]

Preparation and Characterization of the Nanoplatform for *DJ-1* siRNA Delivery to the Ovarian Cancer Cells

siRNA delivery to the cancer cells is significantly hindered by a number of factors including its nuclease degradation in serum and electrostatic repulsion by the negatively charged cellular membrane.[35] To facilitate intracellular siRNA delivery and achieve the efficient suppression of *DJ-1* mRNA, we constructed a dendrimer-based nanoplatform targeting the ovarian cancer cells (Figure 2). Due to a high positively charged surface, the amine-terminated PPIG4 dendrimers were able to effectively complex negatively charged siRNA molecules through electrostatic interactions (Figure 3B).[21, 22, 26] To minimize toxicity and enhance biocompatibility, the positively-charged PPIG4-siRNA complexes (ζ = +23.03 ± 2.22 mV) were modified with heterobifunctional PEG molecules by coupling NHS ester groups of PEG to the primary amino groups of the dendrimers (Figure 2).[21, 23, 29, 30] As a result of this modification, the average zeta potential value of the PPIG4-siRNA complexes decreased from +23.03 ± 2.22 mV to + 6.44 ± 2.14 mV indicating that the majority of primary amine groups, which could cause cellular membrane damage, were successfully PEGylated. The toxicity study validated that in comparison to non-modified PPIG4 complexes loaded with scrambled siRNA, the PEGylate complexes do not compromise cellular viability (Figure 3C). Finally, to improve nanoplatform specificity to the ovarian cancer cells, degradation-resistant LHRH peptide was attached to the distal end of PEG, by coupling the maleimide group of PEG to cysteine thiol presented in the LHRH sequence (Figure 2).[21–23] The employed targeting moiety exploits preferential overexpression of LHRH receptors on the extracellular surface of the various ovarian cancer cells, including A2780/CDDP, ES2 and IGOV-1 cells.[20–23, 36–41] Recently, we reported that gynecologic (both primary and metastatic) tumors, obtained from patients with advanced ovarian carcinoma, overexpressed LHRH receptors.[42] Conversely, in the majority of healthy organs,

there were no detectable levels of LHRH receptors.[42] Moreover, our previous reports confirmed that nanoplatforms equipped with LHRH peptide can efficiently deliver siRNA molecules to LHRH-positive cancer cells both *in vitro* and *in vivo*.[21–25] Following the modification steps, we determined hydrodynamic size of the constructed siRNA nanoplatform, which turned out to be 147.8 ± 11.0 nm (Figure 3D). The LHRH-targeted, nanoplatform loaded with the scrambled siRNA, did not compromise viability (Figure 3C), proliferation (Figure S2) and DJ-1 mRNA expression (Figure S3) of ovarian cancer cells, indicating that the prepared siRNA delivery system is non-toxic.

To assess the cellular internalization efficiency of the LHRH-equipped nanoplatform and investigate the role of LHRH peptide as a targeting ligand, LHRH receptor-positive (A2780/CDDP, ES2 and IGROV1)[39–41] and LHRH receptor-negative (SKOV3)[39] ovarian cancer cell lines were incubated with the delivery system containing fluorescently labeled siRNA for 24 h. According to the flow cytometry measurements, fluorescence signal was detected in more than 85% A2780/CDDP, ES2 and IGROV1 cells, thus reflecting high internalization efficiency of the nanoplatform into the LHRH receptor-positive ovarian cancer cell lines (Figure 4). In contrast, only 50% LHRH receptor-negative SKOV3 cells were transfected with the LHRH-targeted nanoplatform (Figure S4), indicating preferential uptake of the constructed nanoplatform by the LHRH-positive cancer cells.

The qPCR analysis revealed that the 1μM *DJ-1* siRNA delivered by the prepared nanoplatform downregulated the expression of targeted mRNA to 22%, 15% and 14% of the basal level in A2780/CDDP, ES2 and IGROV1 cells at 24 h post-transfection, respectively (Figure 5A). In case of ES2 and IGROV1 cells, the suppression of *DJ-1* mRNA levels persisted 96 h following a single transfection. In contrast, the intracellular level of *DJ-1* mRNA in the CDDP-resistant A2780 cells was gradually restored under the same experimental conditions, recovering from the 22% after 24 h to 90% of the basal level at 96 h. This finding indicates that A2780/CDDP cells rely on DJ-1 protein for continued growth and CDDP chemoresistance. The western immunoblotting analysis further confirmed the similar trend in DJ-1 protein expression at the studied time points (Figure 5B). The suppression of DJ-1 protein in both ES2 and IGROV1 cells remained persistent (<5% of the basal level) at 96 h after a single transfection. Contrary to the qPCR data, the western blot analysis revealed that the steady-state protein levels of DJ-1 in A2780/CDDP cells 24 h after DJ-1 suppression were decreased to 11% of the basal DJ-1 protein concentrations, and after 96 h only recovered to 54%, indicating that the intracellular amount of DJ-1 protein remained substantially suppressed at this time point. The discrepancy between mRNA and protein levels is due to the finite amount of time between mRNA production and functional protein assembly.

To achieve an efficient silencing of *DJ-1* mRNA and the corresponding protein, 1 μM siRNA therapeutic dose has been chosen based on the experimental observation. The qPCR data revealed a dose dependent suppression of *DJ-1* mRNA in the ovarian cancer cells 24 h after transfection with the constructed nanoplatform containing various siRNA concentrations and only 1 μM siRNA resulted in greater than 85% mRNA silencing (Figure S5). The selected relatively high dose of *DJ-1* siRNA is in a good agreement with a previously published report, which indicated that complete suppression of *DJ-1* mRNA was only achieved after

cells incubation for 36 h with 2 μM siRNA encapsulated in the commercially available Oligofectamine.[43] Our *in vivo* experiments further confirmed that *DJ-1* siRNA (1.1 mg/kg) delivered by the constructed nanoplatform after intravenous injection into mice bearing subcutaneous ovarian cancer xenograft can substantially suppress the targeted DJ-1 protein in cancer tissue (Figure S6). The employed siRNA dosage is in good agreement with the previous clinical trials, which validated that administration of 1.5 mg/kg formulated siRNA was well tolerated and has antitumor activity.[44]

Effect of DJ-1 Protein Suppression on Cancer Cells Proliferation, Viability and Migration

By measuring cell growth in real time with the xCELLigence System, it was demonstrated that suppression of DJ-1 protein expression with siRNA, delivered by the constructed nanoplatform, dramatically impaired proliferation of the employed ovarian cancer cells as compared to the controls (Figure 6). It is worth mentioning that knockdown of DJ-1 expression by siRNA produced a superior reduction in ovarian cancer cell proliferation than CDDP alone at the corresponding IC_{50} concentrations (Figure 6). Finally, the combinatorial therapeutic approach led to the most pronounced inhibition of proliferation in all the studied cell lines, outperforming both siRNA-mediated DJ-1 knockdown and CDDP treatment alone (Figure 6). A decrease in cellular proliferation can be initially seen at ~48 h after the addition of siRNA to the culture media in all cell lines. The observed effect is consistent with the qPCR and western blot data (Figure 5), which validate the substantial suppression of both *DJ-1* mRNA and protein levels at the ~48 h time point. Furthermore, the inhibitory effect of DJ-1 suppression on cell proliferation was most pronounced at 72 and 96 h post-treatment, where DJ-1 is predicted to have 3–4 half-lives of turn over, [45] achieving maximal intracellular suppression.

In addition to the real-time proliferation studies, we also evaluated the effect of DJ-1 suppression alone or in combination with CDDP on the viability of cancer cells using Calcein AM assay at 72 and 96 h post-transfection. As shown in Figure 7, siRNA-mediated silencing of DJ-1 protein reduced viability of all the studied ovarian cancer cell lines. It is noteworthy that the decrease in viability was the most pronounced in the CDDP-resistant ovarian cancer cells (A2780/CDDP), which are characterized by the highest overexpression of the DJ-1 protein (Figure 3A). In contrast, non-resistant IGROV cells, which exhibit the lowest DJ-1 protein expression (Figure 3A), were found to be the least sensitive to the siRNA treatment. Thus, viability of A2780/CDDP cells decreased from 100% to 32.3% 96 h post-transfection relative to the control (Figure 7). In contrast, the viability of ES-2 ovarian cancer cells with low resistance to CDDP and non-resistant IGROV-1 cells was 52.0 and 77.4% following the same treatment, respectively (Figure 7). Combination of *DJ-1* siRNA and CDDP lead to further decrease in cellular viability down to 14.3, 16.3 and 24.2% for A2780/CDDP, ES-2, and IGROV-1 respectively. These results revealed that higher cellular levels of DJ-1 could increase the survival of the ovarian cancer cells and enhance their resistance to platinum-based chemotherapeutic drugs. Therefore, the siRNA-mediated silencing of DJ-1 can efficiently inhibit both cancer cell survival and proliferation all the while improving their sensitivity to chemotherapy. The obtained data is consistent with the previous reports, which demonstrated that DJ-1 protein suppression in cancer cells can effectively enhance the efficacy of the anti-cancer therapies.[21, 46] For example, Zhang *et al.*

reported that the sensitivity of adriamycin resistance MCF-7 breast cancer cells to chemotherapy was significantly improved following DJ-1 knockdown. In another study, Schumann *et al.* demonstrated that the therapeutic efficacy of the photodynamic therapy for ovarian cancer treatment was substantially enhanced through the siRNA-mediated inhibition of the DJ-1 protein and this effect was more pronounced in A2780/AD cells than in ES2 cells, wherein former cells are characterized by higher basal levels of DJ-1 protein.[21]

Because intracellular DJ-1 is known to regulate the process of cancer cell migration,[47, 48] we also employed the wound healing assay to assess an effect of siRNA-mediated DJ-1 knockdown alone or in combination with CDDP on the migration capacity of ovarian cancer cells. Immediately after initiating an appropriate treatment, a scratch was made in the cell monolayer and migration of cancer cells to the wound area was monitored at different time points. In comparison to non-treated cells, cancer cells exposed to CDDP alone demonstrated some decrease in migration (Figure 8). Furthermore, both DJ-1 suppression alone and combinatorial therapy inhibited ovarian cancer cell motility. The obtained results indicated that not only siRNA-induced DJ-1 suppression in combination with CDDP is capable of a substantial reduction in ovarian cancer cell proliferation and viability, but it also can suppress their migration and thus inhibit the potential metastasis development. These results are in a good agreement with the previous studies reported by He *et al.*, which indicated that the cellular levels of DJ-1 correlate with migration and invasion of pancreatic ductal adenocarcinoma cells and knockdown of DJ-1 expression can inhibit metastasis *in vivo*.[47] In another study, Pei *et al.* also reported that high expression of DJ-1 in nasopharyngeal carcinoma enhances migratory properties of cancer cells *in vitro* and plays a significant role in lymph node metastasis.[48] Finally, Feng *et al.* reported that overexpression of DJ-1 promotes migration of human glioma cells possibly through DJ-1-induced down regulation of phosphatase PTEN.[49]

Role of the DJ-1 Protein Suppression in the Combinatorial Therapeutic Approach

The observed superior anticancer effect of the combinatorial treatment is related to the fact that the employed individual therapies can target multiple pathways that drive ovarian cancer progression. It is established that CDDP halts the growth of ovarian carcinomas primarily through the induction of DNA crosslinks and inhibition of cellular division.[50] Unlike CDDP, the siRNA-mediated DJ-1 silencing can concurrently affect several pathways that ovarian cancer cells use for their proliferation, survival, migration and resistance to the chemotherapeutic agents (Figure 1). We sought to interrogate molecular underpinnings of the DJ-1 knockdown effects in the treatment of the ovarian cancer cells. Firstly, DJ-1 protein plays a vital role in the proliferation and growth of cancer cells through direct mediation of the Akt pathway.[14, 51] It binds to PTEN thereby decreasing PTEN activity and increasing phosphorylation of protein kinase Akt, thus promoting unregulated proliferation of cancer cells (Figure 1A).[9] Consequently, an increase in DJ-1 basal levels is associated with enhanced aggressiveness of the cancer. For example, Wang *et al.* revealed that the overexpression of DJ-1 in laryngeal squamous carcinoma cells is correlated with increased expression of phosphorylated Akt (p-Akt) and the high intracellular levels of DJ-1 can accelerate proliferation rate, increase the invasiveness and migration capacity, and reduce apoptosis, by activating the PI3K/Akt/mTOR signaling axis.[52] It has been confirmed that the

proliferation rate of DJ-1-overexpressing SNU-46-D1 cells was faster than normal SNU-46 cells. Through the modulation of this signaling axis DJ-1 has also been implicated in tumor growth and progression by upregulating hypoxia-inducible factor-1 (HIF1) protecting the cells against hypoxia induced apoptosis. Vasseur et. al. reported a link between DJ-1 and Akt, mTOR, and HIF1 activation as well as inhibition of p53-mediated cellular apoptosis in tumor progression.[53] In our study, immunoblot analysis validated that suppression of DJ-1 protein expression with siRNA delivered by the prepared nanoplatform, caused substantial decrease in p-Akt levels in all the ovarian cancer cell lines tested (Figure 9A). Consequently, the proliferation and viability of these cells was significantly decreased (Figures 6 and 7). By analyzing perfusions and solid ovarian cancer tumors, Davidson *et al.* validated that DJ-1 is commonly expressed in advanced-stage ovarian carcinoma, but PTEN expression is infrequent. It is assumed that DJ-1 expression could have a prognostic role in ovarian carcinoma, possibly by suppressing the inhibitory action of PTEN on the Akt survival pathway.[10]

Second, DJ-1 could promote cancer cells survival, growth, and contributes, in part, to CDDP resistance by repressing activity of p53 tumor suppressor protein.[15, 54] The cytoprotective function of DJ-1 is related to its ability to sequester p53, therefore inhibiting the apoptotic p53-Bax-caspase pathway and cell cycle arrest functionality (Figure 1B).[1555] The aforementioned Akt signaling pathway is also influenced by the p53 protein activity. Astanehe *et al.* reported that p53 binds to the promoter of PI3K and inhibits its actions, preventing the phosphylation of Akt, thereby decreasing cell proliferation and growth.[56] Using western blot analysis, we assessed a change of p53 protein level in the ovarian cancer cells before and after treatment with the nanoplatform containing *DJ-1* targeted siRNA. A substantial increase in p53 protein expression was found in the all tested cancer cells following siRNA treatment indicating inverse correlation between DJ-1 protein levels and p53 expression (Figure 9B). To further validate the role of DJ-1 suppression in regaining p53 function and the subsequent negative impact on cells proliferation and viability, we assessed caspase activity and cell cycle parameters of the cells in question before and after treatment with *DJ-1* siRNA-NP, CDDP or combinatorial therapy. The siRNA-mediated attenuation of DJ-1 and the consequent increase in p53 expression resulted in blockade of cell cycle progression at the G_0/G_1 phase (Figure 10). When compared to the untreated cells, the G_0/G_1 population of siRNA-treated A2780/AD, ES2 and IGROV-1 cells increased by 43.6, 33.9, and 29.4%, respectively (Figure 10). This result suggests that the A2780/CDDP ovarian cancer cells with the highest basal level of DJ-1 protein are most susceptible to the *DJ-1* siRNA-induced cell cycle arrest. Importantly, this susceptibility declines with decreasing basal levels of DJ-1 as seen in ES2 and IGROV-1 cell lines. Finally, the combinatorial therapy showed the most pronounced effect in blocking cell cycle progression as compared to the standalone *DJ-1* siRNA and CDDP treatments. The number of A2780/AD, ES2 and IGROV-1 cells in the G_0/G_1 phase following combinatorial therapy increased by 52.4, 40.6, and 37.4%, respectively when compared to the untreated cells. To the best of our knowledge, this is the first report demonstrating that the knockdown of DJ-1 protein in ovarian cancer cells results in cell cycle arrest at the G_0/G_1 phase, which likely contributes to the decrease in cell proliferation and viability. Previous studies showed that certain anticancer agents such as curcumin and ellagic acid induced G_0/G_1 cell arrest

through increased p53 levels and caused apoptosis in human bladder and breast cancer cells.[57, 58]

By using caspase assay, we also demonstrated that siRNA-mediated knockdown of DJ-1 protein substantially increased caspase activation in all the tested ovarian cancer cell lines in comparison to the control and CDDP treatment alone (Figure 11A and S7). Our results are in good agreement with the previous report, which indicated that DJ-1 blocks caspase-3 activation by repressing p53 function and therefore, decreasing the Bax protein level.[15] It is important to mention that the detected effect was the most pronounced in A2780/CDDP cells characterized by the highest intracellular level of the DJ-1 protein. Thus, in comparison to non-treated cells, incubation of A2780/CDDP, ES2 and IGROV1 cells with siRNA-NP increased caspase activity by 75.6, 51.1, and 38.3%, respectively (Figure 11A). Finally, combinatorial treatment resulted in further increase of caspase activation by 106.4, 84.9 and 83.6% in A2780/CDDP, ES2 and IGROV1 cells, respectively. The above results provided evidence that siRNA-mediated DJ-1 silencing in ovarian cancer cells inhibits DJ-1 protective function associated with its ability of repressing p53 transcriptional activity, therefore inhibiting the apoptotic p53-Bax-caspase pathway and cell cycle arrest functionality.

One of the main alterations in ovarian cancer cells, compared to nonmalignant ones, is excessive cellular levels of toxic reactive oxygen species (ROS).[59] The cancer cells have developed a ROS defense system to protect themselves from intrinsic oxidative stress and to provide resistance to ROS-induced therapies.[60] Through multiple mechanisms, DJ-1 protein plays an important role in protecting ovarian cancer cells from toxic intracellular ROS and the exogenous ROS generated by various anticancer agents, including CDDP.[61] Therefore, weakening the cellular ROS defense mechanism by siRNA-mediated DJ-1 knockdown may result in ROS-mediated cell death.

DJ-1 has been shown to influence synthesis of the non-enzymatic antioxidant, reduced glutathione (GSH), via upregulation of the rate limiting enzyme glutamate cysteine ligase (GCL) thereby increasing intracellular GSH pool (Figure 1C).[17] Godwin *et al.* reported that ovarian cancer cells with a platinum resistant phenotype have increased intracellular GSH concentration with a linear relationship to resistance.[62] We also verified that platinum-resistant A2780/CDDP cells have the highest basal levels of GSH when compared to the ES2 and IGROV1 cells lines (Figure 11B). Following DJ-1 suppression, intracellular GSH level is decreased by 56.4% in the A2780/CDDP cells where the ES2 and IGROV1 cells were characterized by a 31.6% and 21.7% reduction, respectively (Figure 11B). These data are in good agreement with the published hypothesis that GSH upregulation in platinum-resistant cancer cells and the reliance of these cells on DJ-1 as a cellular GSH mediator. [17, 62]

Additionally, DJ-1 has been reported to directly influence the activity of the oxidative stress-responsive transcription factor NRF2, stabilizing it, therefore inhibiting its association with the ubiquitinase Keap1 and increasing NRF2's transcriptional activity.[63–65] NRF2 plays a critical role in redox regulation within the cell and is responsible for NRF2-regulated GSH recycling via modulating the activity of glutathione reductase as well as transcriptional regulation of a variety of other antioxidant stress response proteins (Figure 1C).[16, 66, 67]

Using western blot analysis, we assessed NRF2 protein levels following siRNA-mediated DJ-1 suppression and found a significant decrease in the amount of NRF2 protein in all the tested cell lines, thus confirming DJ-1's role in NRF2 stabilization (Figure 11C). Clements *et al*. previously revealed that in the absence of intact DJ-1, NRF2 protein is unstable, and transcriptional responses are consequentially decreased - both basally and after induction.[63] Hence, the DJ-1/NRF2 functional axis presents a prospective therapeutic target in cancer treatment and DJ-1 knockdown could contribute to ROS-mediated cell death.

Finally, it has been reported that the redox-sensitive Cys-106 residue of DJ-1 is highly susceptible to hydrogen peroxide (H_2O_2)-induced oxidation and may be responsible for H_2O_2 scavenging.[68] Consistently, DJ-1 has been shown to reduce or prevent H_2O_2-mediated cell death.[43] To evaluate the effect of DJ-1 suppression and CDDP on intracellular H_2O_2 levels, the employed cancer cell lines were subjected to the siRNA-loaded nanoplatform, CDDP or combinatorial treatment. Following DJ-1 suppression, we observed an 81.0% increase in intracellular H_2O_2 in the platinum resistant A2780/CDDP cells and a 63.4% and 46.2% increase in ES2 and IGROV1 cells, respectively (Figure 11D). This data is in agreement with the basal levels of DJ-1 reported in this study, whereby higher levels of DJ-1 in the cells permit a more robust and efficient ROS scavenging.

Similarly, CDDP has been shown to stimulate the production of endogenous ROS.[69] To understand the impact of CDDP on enhanced intracellular ROS generation, all cell lines in question were treated at their respective IC_{50} concentrations. Following the treatment, these cell lines exhibited small increase in ROS, ranging from a 2.02 to 12.32% relative to control (Figure 11D). [69, 70] The elevated ROS seen with CDDP+DJ-1 suppression regimen was greater than the increase in ROS seen in the sole DJ-1 suppression treatment group. Out of all the cell lines the most pronounced ROS elevation occurred in the A2780/CDDP cell line, where the difference between the DJ-1 suppression only and the combinatorial treatment was 28.83% versus 11.36% and 8.45%, seen in the ES2, and IGROV-1 cell lines, respectively (Figure 11D).

The above results revealed that upon DJ-1 suppression there is a reproducible substantial increase in endogenous H_2O_2 as well as a significant decrease of intracellular GSH pool and NRF2 protein. Such alteration in the intercellular ROS (produced as a consequence of a weakened antioxidant defense system) further confirms the reliance of ovarian cancer cells on DJ-1, which acts as a buffer for intracellular ROS. This data is in agreement with our previously published observation of a dramatic increase in endogenous ROS in the DJ-1-overexpressing A2780/AD (Adriamycin-resistant) cells upon the protein's depletion in combination with ROS-inducing photodynamic therapy.[21]

CONCLUSIONS

A dendrimer-based, LHRH-targeted drug delivery system was constructed to deliver *DJ-1* targeted siRNA to ovarian cancer cells in combination with CDDP. The DJ-1 nanoplatform showed sufficient cellular uptake to achieve therapeutic *DJ-1* mRNA suppression levels. The silencing of DJ-1 provided a therapeutic approach that encompassed three ovarian cancer survival pathways that intersect with CDDP's mechanism of action: (i) increasing apoptosis;

(ii) decreasing cellular proliferation; and (iii) increasing intracellular ROS levels. In this study, we found that DJ-1 suppression in combination with CDDP treatment is a feasible therapeutic modality, and offers a new prospective avenue for the treatment of CDDP-resistant ovarian cancer. The current work established a foundation for subsequent evaluation of the developed combinatorial therapy in animal models with either subcutaneous or orthotopic ovarian cancer tumors.

Supplementary Material

Refer to Web version on PubMed Central for supplementary material.

Acknowledgments

This research was supported in part by grants from NIH/NBIB (1R15EB020351-01A1), PhRMA, the Medical Research Foundation of Oregon Health and Science University, OSU General Research Fund and OSU College of Pharmacy to O.T., and NIH/NIGMS (R01GM108975) to O.K.

References

1. McCorkle R, Pasacreta J, Tang ST. The Silent Killer: Psychological Issues in Ovarian Cancer. Holist Nurs Pract. 2003; 17:300–308. [PubMed: 14650572]
2. Cancer Facts and Figures. American Cancer Society; 2016. http://www.cancer.org/research/cancerfactsstatistics/cancerfactsfigures2014/
3. Bristow RE, Tomacruz RS, Armstrong DK, Trimble EL, Montz FJ. Survival Effect of Maximal Cytoreductive Surgery for Advanced Ovarian Carcinoma During the Platinum Era: A Meta-Analysis. J Clin Oncol. 2002; 20:1248–1259. [PubMed: 11870167]
4. Lim MC, Kang S, Lee KS, Han SS, Park SJ, Seo SS, Park SY. The Clinical Significance of Hepatic Parenchymal Metastasis in Patients with Primary Epithelial Ovarian Cancer. Gynecol Oncol. 2009; 112:28–34. [PubMed: 19010521]
5. Al-Lazikani B, Banerji U, Workman P. Combinatorial Drug Therapy for Cancer in the Post-Genomic Era. Nat Biotechnol. 2012; 30:679–692. [PubMed: 22781697]
6. DeVita VT Jr, Young RC, Canellos GP. Combination Versus Single Agent Chemotherapy: A Review of the Basis for Selection of Drug Treatment of Cancer. Cancer. 1975; 35:98–110. [PubMed: 162854]
7. Agarwal R, Kaye SB. Ovarian Cancer: Strategies for Overcoming Resistance to Chemotherapy. Nat Rev Cancer. 2003; 3:502–516. [PubMed: 12835670]
8. Ariga H, Takahashi-Niki K, Kato I, Maita H, Niki T, Iguchi-Ariga SM. Neuroprotective Function of DJ-1 in Parkinson's Disease. Oxid Med Cell Longev. 2013; 2013:683920. [PubMed: 23766857]
9. Cao J, Lou S, Ying M, Yang B. Dj-1 as a Human Oncogene and Potential Therapeutic Target. Biochem Pharmacol. 2015; 93:241–250. [PubMed: 25498803]
10. Davidson B, Hadar R, Schlossberg A, Sternlicht T, Slipicevic A, Skrede M, Risberg B, Florenes VA, Kopolovic J, Reich R. Expression and Clinical Role of DJ-1, a Negative Regulator of Pten, in Ovarian Carcinoma. Hum Pathol. 2008; 39:87–95. [PubMed: 17949781]
11. Yuen HF, Chan YP, Law S, Srivastava G, El-Tanani M, Mak TW, Chan KW. DJ-1 Could Predict Worse Prognosis in Esophageal Squamous Cell Carcinoma. Cancer Epidemiol Biomarkers Prev. 2008; 17:3593–3602. [PubMed: 19064576]
12. Zeng HZ, Qu YQ, Zhang WJ, Xiu B, Deng AM, Liang AB. Proteomic Analysis Identified DJ-1 as a Cisplatin Resistant Marker in Non-Small Cell Lung Cancer. Int J Mol Sci. 2011; 12:3489–3499. [PubMed: 21747690]
13. Hlobilkova A, Knillova J, Bartek J, Lukas J, Kolar Z. The Mechanism of Action of the Tumour Suppressor Gene PTEN. Biomed Pap Med Fac Univ Palacky Olomouc Czech Repub. 2003; 147:19–25. [PubMed: 15034601]

14. Kim RH, Peters M, Jang Y, Shi W, Pintilie M, Fletcher GC, DeLuca C, Liepa J, Zhou L, Snow B, Binari RC, Manoukian AS, Bray MR, Liu FF, Tsao MS, Mak TW. DJ-1, a Novel Regulator of the Tumor Suppressor PTEN. Cancer Cell. 2005; 7:263–273. [PubMed: 15766664]
15. Fan J, Ren H, Jia N, Fei E, Zhou T, Jiang P, Wu M, Wang G. DJ-1 Decreases Bax Expression through Repressing P53 Transcriptional Activity. J Biol Chem. 2008; 283:4022–4030. [PubMed: 18042550]
16. Liu C, Chen Y, Kochevar IE, Jurkunas UV. Decreased DJ-1 Leads to Impaired Nrf2-Regulated Antioxidant Defense and Increased UV-A-Induced Apoptosis in Corneal Endothelial Cells. Invest Ophthalmol Vis Sci. 2014; 55:5551–5560. [PubMed: 25082883]
17. Zhou W, Freed CR. DJ-1 up-Regulates Glutathione Synthesis During Oxidative Stress and Inhibits A53t Alpha-Synuclein Toxicity. J Biol Chem. 2005; 280:43150–43158. [PubMed: 16227205]
18. Chen Y, Kang M, Lu W, Guo Q, Zhang B, Xie Q, Wu Y. DJ-1, a Novel Biomarker and a Selected Target Gene for Overcoming Chemoresistance in Pancreatic Cancer. J Cancer Res Clin Oncol. 2012; 138:1463–1474. [PubMed: 22526154]
19. Harries M, Gore M. Part I: Chemotherapy for Epithelial Ovarian Cancer-Treatment at First Diagnosis. Lancet Oncol. 2002; 3:529–536. [PubMed: 12217790]
20. Li X, Taratula O, Taratula O, Schumann C, Minko T. LHRH-Targeted Drug Delivery Systems for Cancer Therapy. Mini-Rev Med Chem. 2016; 16
21. Schumann C, Taratula O, Khalimonchuk O, Palmer AL, Cronk LM, Jones CV, Escalante CA. ROS-Induced Nanotherapeutic Approach for Ovarian Cancer Treatment Based on the Combinatorial Effect of Photodynamic Therapy and DJ-1 Gene Suppression. Nanomedicine. 2015; 11:1961–1970. [PubMed: 26238076]
22. Shah V, Taratula O, Garbuzenko OB, Taratula OR, Rodriguez-Rodriguez L, Minko T. Targeted Nanomedicine for Suppression of CD44 and Simultaneous Cell Death Induction in Ovarian Cancer: An Optimal Delivery of Sirna and Anticancer Drug. Clin Cancer Res. 2013; 19:6193–6204. [PubMed: 24036854]
23. Taratula O, Garbuzenko OB, Kirkpatrick P, Pandya I, Savla R, Pozharov VP, He HX, Minko T. Surface-Engineered Targeted PPI Dendrimer for Efficient Intracellular and Intratumoral siRNA Delivery. J Control Release. 2009; 140:284–293. [PubMed: 19567257]
24. Taratula O, Garbuzenko O, Savla R, Wang YA, He H, Minko T. Multifunctional Nanomedicine Platform for Cancer Specific Delivery of Sirna by Superparamagnetic Iron Oxide Nanoparticles-Dendrimer Complexes. Curr Drug Deliv. 2011; 8:59–69. [PubMed: 21034421]
25. Taratula O, Kuzmov A, Shah M, Garbuzenko OB, Minko T. Nanostructured Lipid Carriers as Multifunctional Nanomedicine Platform for Pulmonary Co-Delivery of Anticancer Drugs and siRNA. J Control Release. 2013; 171:349–357. [PubMed: 23648833]
26. Taratula O, Savla R, He H, Minko T. Poly (Propyleneimine) Dendrimers as Potential siRNA Delivery Nanocarrier: From Structure to Function. Int J Nanotechnol. 2010; 8:36–52.
27. Taratula O, Schumann C, Naleway MA, Pang AJ, Chon KJ. A Multifunctional Theranostic Platform Based on Phthalocyanine-Loaded Dendrimer for Image-Guided Drug Delivery and Photodynamic Therapy. Mol Pharm. 2013; 10:3946–3958. [PubMed: 24020847]
28. Taratula O, Doddapaneni BS, Schumann C, Li X, Bracha S, Milovancev M, Alani A, Taratula O. Naphthalocyanine-Based Biodegradable Polymeric Nanoparticles for Image-Guided Combinatorial Phototherapy. Chem Mater. 2015; 27:6155–6165.
29. Taratula O, Patel M, Schumann C, Naleway MA, Pang AJ, He H. Phthalocyanine-Loaded Graphene Nanoplatform for Imaging-Guided Combinatorial Phototherapy. Int J Nanomedicine. 2015; 10:2347–2362. [PubMed: 25848255]
30. Schumann C, Taratula O, Khalimonchuk O, Palmer AL, Cronk LM, Jones CV, Escalante CA, Taratula O. ROS-Induced Nanotherapeutic Approach for Ovarian Cancer Treatment Based on the Combinatorial Effect of Photodynamic Therapy and DJ-1 Gene Suppression. Nanomedicine. 2015; 11:1961–1970. [PubMed: 26238076]
31. Dani RK, Schumann C, Taratula O. Temperature-Tunable Iron Oxide Nanoparticles for Remote-Controlled Drug Release. AAPS PharmSciTech. 2014; 15:963–972. [PubMed: 24821220]

32. Arif T, Vasilkovsky L, Refaely Y, Konson A, Shoshan-Barmatz V. Silencing VDAC1 Expression by siRNA Inhibits Cancer Cell Proliferation and Tumor Growth in Vivo. Mol Ther Nucleic Acids. 2014; 3:e159. [PubMed: 24781191]
33. Beaufort CM, Helmijr JC, Piskorz AM, Hoogstraat M, Ruigrok-Ritstier K, Besselink N, Murtaza M, van IWF, Heine AA, Smid M, Koudijs MJ, Brenton JD, Berns EM, Helleman J. Ovarian Cancer Cell Line Panel (OCCP): Clinical Importance of in Vitro Morphological Subtypes. PLoS One. 2014; 9:e103988. [PubMed: 25230021]
34. Benard J, Da Silva J, De Blois MC, Boyer P, Duvillard P, Chiric E, Riou G. Characterization of a Human Ovarian Adenocarcinoma Line, IGROV1, in Tissue Culture and in Nude Mice. Cancer Res. 1985; 45:4970–4979. [PubMed: 3861241]
35. Borna H, Imani S, Iman M, Azimzadeh Jamalkandi S. Therapeutic Face of RNAi: In Vivo Challenges. Expert Opin Biol Ther. 2015; 15:269–285. [PubMed: 25399911]
36. Arencibia JM, Bajo AM, Schally AV, Krupa M, Chatzistamou I, Nagy A. Effective Treatment of Experimental ES-2 Human Ovarian Cancers with a Cytotoxic Analog of Luteinizing Hormone-Releasing Hormone AN-207. Anticancer Drugs. 2002; 13:949–956. [PubMed: 12394258]
37. Volker P, Grundker C, Schmidt O, Schulz KD, Emons G. Expression of Receptors for Luteinizing Hormone-Releasing Hormone in Human Ovarian and Endometrial Cancers: Frequency, Autoregulation, and Correlation with Direct Antiproliferative Activity of Luteinizing Hormone-Releasing Hormone Analogues. Am J Obstetr Gynecol. 2002; 186:171–179.
38. Khan AR, Magnusson JP, Watson S, Grabowska AM, Wilkinson RW, Alexander C, Pritchard D. Camptothecin Prodrug Block Copolymer Micelles with High Drug Loading and Target Specificity. Polym Chem. 2014; 5:5320–5329.
39. Dharap SS, Qiu B, Williams GC, Sinko P, Stein S, Minko T. Molecular Targeting of Drug Delivery Systems to Ovarian Cancer by BH3 and LHRH Peptides. J Control Release. 2003; 91:61–73. [PubMed: 12932638]
40. Ho MN, Delgado CH, Owens GA, Steller MA. Insulin-Like Growth Factor-II Participates in the Biphasic Effect of a Gonadotropin-Releasing Hormone Agonist on Ovarian Cancer Cell Growth. Fertil Steril. 1997; 67:870–876. [PubMed: 9130892]
41. Keller G, Schally AV, Gaiser T, Nagy A, Baker B, Halmos G, Engel JB. Receptors for Luteinizing Hormone Releasing Hormone (LHRH) Expressed in Human Non-Hodgkin's Lymphomas Can Be Targeted for Therapy with the Cytotoxic LHRH Analogue AN-207. Eur J Cancer. 2005; 41:2196–2202. [PubMed: 16182122]
42. Shah V, Taratula O, Garbuzenko OB, Taratula OR, Rodriguez-Rodriguez LTM. Targeted Nanomedicine for Suppression of CD44 and Simultaneous Cell Death Induction in Ovarian Cancer: An Optimal Delivery of siRNA and Anticancer Drug. Clin Cancer Res. 2013; 19:6193–6204. [PubMed: 24036854]
43. Taira T, Saito Y, Niki T, Iguchi-Ariga SM, Takahashi K, Ariga H. DJ-1 Has a Role in Antioxidative Stress to Prevent Cell Death. EMBO Rep. 2004; 5:213–218. [PubMed: 14749723]
44. Tabernero J, Shapiro GI, LoRusso PM, Cervantes A, Schwartz GK, Weiss GJ, Paz-Ares L, Cho DC, Infante JR, Alsina M, Gounder MM, Falzone R, Harrop J, White AC, Toudjarska I, Bumcrot D, Meyers RE, Hinkle G, Svrzikapa N, Hutabarat RM, Clausen VA, Cehelsky J, Nochur SV, Gamba-Vitalo C, Vaishnaw AK, Sah DW, Gollob JA, Burris HA 3rd. First-in-Humans Trial of an RNA Interference Therapeutic Targeting VEGF and KSP in Cancer Patients with Liver Involvement. Cancer Discov. 2013; 3:406–417. [PubMed: 23358650]
45. Rannikko EH, Vesterager LB, Shaik JH, Weber SS, Cornejo Castro EM, Fog K, Jensen PH, Kahle PJ. Loss of DJ-1 Protein Stability and Cytoprotective Function by Parkinson's Disease-Associated Proline-158 Deletion. J Neurochem. 2013; 125:314–327. [PubMed: 23241025]
46. Zhang GQ, He C, Tao L, Liu F. Role of DJ-1 siRNA in Reverse Sensitivity of Breast Cancer Cells to Chemotherapy and Its Possible Mechanism. Int J Clin Exp Pathol. 2015; 8:6944–6951. [PubMed: 26261582]
47. He X, Zheng Z, Li J, Ben Q, Liu J, Zhang J, Ji J, Yu B, Chen X, Su L, Zhou L, Liu B, Yuan Y. DJ-1 Promotes Invasion and Metastasis of Pancreatic Cancer Cells by Activating SRC/ERK/uPA. Carcinogenesis. 2012; 33:555–562. [PubMed: 22223849]

48. Pei XJ, Wu TT, Li B, Tian XY, Li Z, Yang QX. Increased Expression of Macrophage Migration Inhibitory Factor and DJ-1 Contribute to Cell Invasion and Metastasis of Nasopharyngeal Carcinoma. Int J Med Sci. 2014; 11:106–115. [PubMed: 24396292]
49. Fang M, Zhong X, Du B, Lin C, Luo F, Tang L, Chen J. Role of DJ-1 Induced PTEN Downregulation in Migration and Invasion of Human Glioma Cells. Chin J Cancer. 2010; 29:988–994. [PubMed: 21114918]
50. Dasari S, Tchounwou PB. Cisplatin in Cancer Therapy: Molecular Mechanisms of Action. Eur J Pharmacol. 2014; 740:364–378. [PubMed: 25058905]
51. Kim YC, Kitaura H, Taira T, Iguchi-Ariga SM, Ariga H. Oxidation of DJ-1-Dependent Cell Transformation through Direct Binding of DJ-1 to PTEN. Int J Oncol. 2009; 35:1331–1341. [PubMed: 19885556]
52. Wang B, Qin H, Wang Y, Chen W, Luo J, Zhu X, Wen W, Lei W. Effect of DJ-1 Overexpression on the Proliferation, Apoptosis, Invasion and Migration of Laryngeal Squamous Cell Carcinoma SNU-46 Cells through PI3K/AKT/mTOR. Oncol Rep. 2014; 32:1108–1116. [PubMed: 24969178]
53. Vasseur S, Afzal S, Tardivel-Lacombe J, Park DS, Iovanna JL, Mak TW. DJ-1/Park7 Is an Important Mediator of Hypoxia-Induced Cellular Responses. Proc Natl Acad Sci U S A. 2009; 106:1111–1116. [PubMed: 19144925]
54. Chiang MF, Chou PY, Wang WJ, Sze CI, Chang NS. Tumor Suppressor WWOX and P53 Alterations and Drug Resistance in Glioblastomas. Front Oncol. 2013; 3:43. [PubMed: 23459853]
55. Kato I, Maita H, Takahashi-Niki K, Saito Y, Noguchi N, Iguchi-Ariga SM, Ariga H. Oxidized DJ-1 Inhibits P53 by Sequestering p53 from Promoters in a DNA-Binding Affinity-Dependent Manner. Mol Cell Biol. 2013; 33:340–359. [PubMed: 23149933]
56. Astanehe A, Arenillas D, Wasserman WW, Leung PC, Dunn SE, Davies BR, Mills GB, Auersperg N. Mechanisms Underlying P53 Regulation of PIK3CA Transcription in Ovarian Surface Epithelium and in Ovarian Cancer. J Cell Sci. 2008; 121:664–674. [PubMed: 18270270]
57. Li TM, Chen GW, Su CC, Lin JG, Yeh CC, Cheng KC, Chung JG. Ellagic Acid Induced p53/p21 Expression, G1 Arrest and Apoptosis in Human Bladder Cancer T24 Cells. Anticancer Res. 2005; 25:971–979. [PubMed: 15868936]
58. Choudhuri T, Pal S, Agwarwal ML, Das T, Sa G. Curcumin Induces Apoptosis in Human Breast Cancer Cells through p53-Dependent Bax Induction. FEBS Lett. 2002; 512:334–340. [PubMed: 11852106]
59. Liou GY, Storz P. Reactive Oxygen Species in Cancer. Free Radic Res. 2010; 44:479–496. [PubMed: 20370557]
60. Takemoto H, Ishii A, Miyata K, Nakanishi M, Oba M, Ishii T, Yamasaki Y, Nishiyama N, Kataoka K. Polyion Complex Stability and Gene Silencing Efficiency with a siRNA-Grafted Polymer Delivery System. Biomaterials. 2010; 31:8097–8105. [PubMed: 20692701]
61. Lev N, Ickowicz D, Melamed E, Offen D. Oxidative Insults Induce DJ-1 Upregulation and Redistribution: Implications for Neuroprotection. Neurotoxicology. 2008; 29:397–405. [PubMed: 18377993]
62. Godwin AK, Meister A, O'Dwyer PJ, Huang CS, Hamilton TC, Anderson ME. High Resistance to Cisplatin in Human Ovarian Cancer Cell Lines Is Associated with Marked Increase of Glutathione Synthesis. Proc Natl Acad Sci USA. 1992; 89:3070–3074. [PubMed: 1348364]
63. Clements CM, McNally RS, Conti BJ, Mak TW, Ting JP. DJ-1, a Cancer- and Parkinson's Disease-Associated Protein, Stabilizes the Antioxidant Transcriptional Master Regulator Nrf2. Proc Natl Acad Sci USA. 2006; 103:15091–15096. [PubMed: 17015834]
64. Malhotra D, Thimmulappa R, Navas-Acien A, Sandford A, Elliott M, Singh A, Chen L, Zhuang X, Hogg J, Pare P, Tuder RM, Biswal S. Expression of Concern: Decline in Nrf2-Regulated Antioxidants in Chronic Obstructive Pulmonary Disease Lungs Due to Loss of Its Positive Regulator, DJ-1. Am J Respir Crit Care Med. 2008; 178:592–604. [PubMed: 18556627]
65. Wilson MA. The Role of Cysteine Oxidation in DJ-1 Function and Dysfunction. Antioxid Redox Signal. 2011; 15:111–122. [PubMed: 20812780]
66. Harvey CJ, Thimmulappa RK, Singh A, Blake DJ, Ling G, Wakabayashi N, Fujii J, Myers A, Biswal S. Nrf2-Regulated Glutathione Recycling Independent of Biosynthesis Is Critical for Cell Survival During Oxidative Stress. Free Radic Biol Med. 2009; 46:443–453. [PubMed: 19028565]

67. Ma Q. Role of Nrf2 in Oxidative Stress and Toxicity. Ann Rev Pharmacol Toxicol. 2013; 53:401–426. [PubMed: 23294312]

68. Kinumi T, Kimata J, Taira T, Ariga H, Niki E. Cysteine-106 of DJ-1 Is the Most Sensitive Cysteine Residue to Hydrogen Peroxide-Mediated Oxidation in Vivo in Human Umbilical Vein Endothelial Cells. Biochem Biophys Res Commun. 2004; 317:722–728. [PubMed: 15081400]

69. Kim HJ, Lee JH, Kim SJ, Oh GS, Moon HD, Kwon KB, Park C, Park BH, Lee HK, Chung SY, Park R, So HS. Roles of NADPH Oxidases in Cisplatin-Induced Reactive Oxygen Species Generation and Ototoxicity. J Neurosci. 2010; 30:3933–3946. [PubMed: 20237264]

70. Marullo R, Werner E, Degtyareva N, Moore B, Altavilla G, Ramalingam SS, Doetsch PW. Cisplatin Induces a Mitochondrial-ROS Response That Contributes to Cytotoxicity Depending on Mitochondrial Redox Status and Bioenergetic Functions. PLoS One. 2013; 8:e81162. [PubMed: 24260552]

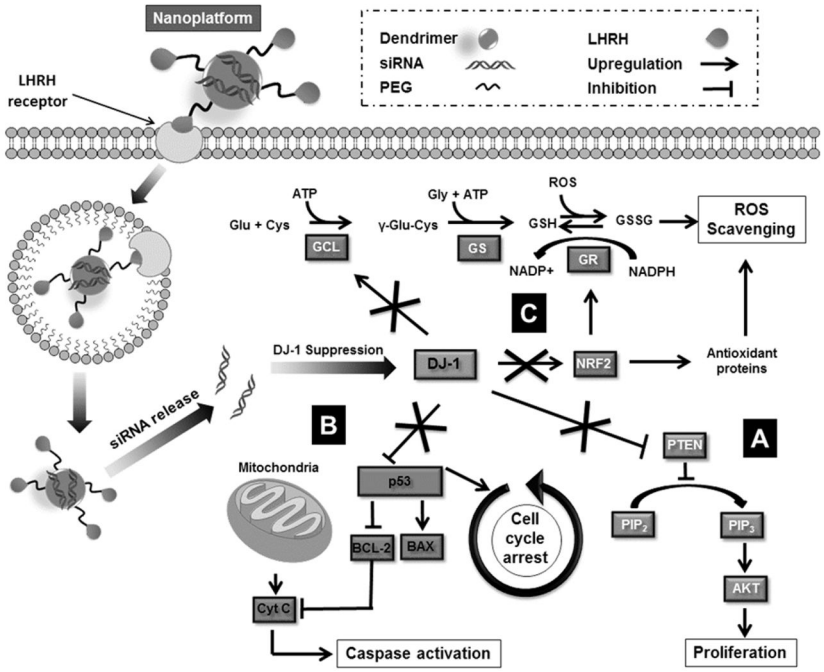

Figure 1.

Schematic illustration of the dendrimer-based nanoplatform for targeted delivery of *DJ-1* siRNA to the ovarian cancer cells via LHRH receptor-mediated endocytosis and the role of siRNA-induced suppression of DJ-1 protein in the combinatorial treatment. siRNA-mediated knockdown prevents DJ-1 protein from **(A)** inhibiting the PTEN expression, thereby promoting phosphorylation of Akt and activating cell proliferation and migration; **(B)** suppressing p53 transcriptional activity, therefore inhibiting the apoptotic p53-Bax-caspase pathway and cell cycle arrest functionality; **(C)** protecting cancer cells from intrinsic oxidative stress and the consequent ROS-mediated apoptosis. DJ-1 facilitates GSH synthesis via upregulation of the rate-limiting enzyme glutamate cysteine ligase (GCL). In addition, DJ-1 stabilizes NRF2, which is responsible for both GSH recycling via modulating the activity of glutathione reductase (GR) and transcriptional activation of various antioxidant proteins.

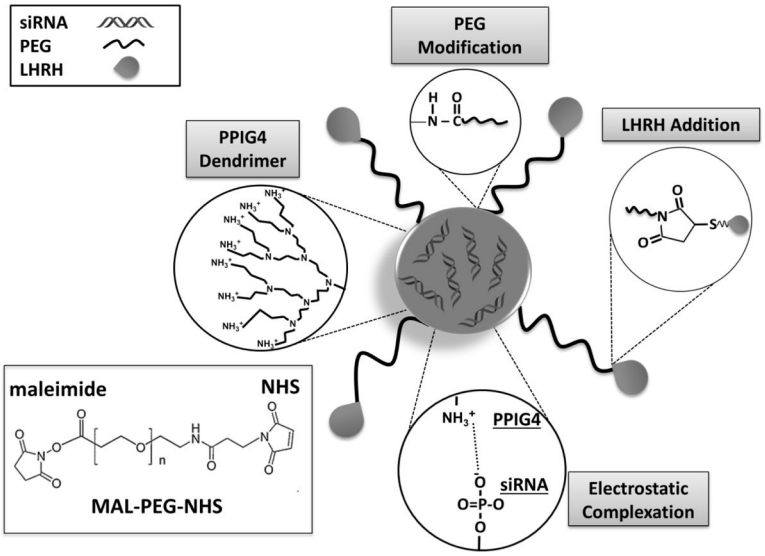

Figure 2.

Schematic representation of the LHRH-targeted, PPIG4 dendrimer-based nanoplatform for siRNA delivery. The developed nanoparticles contain four components: 1) *DJ-1* siRNA, as suppressors of the corresponding mRNA in the ovarian cancer cells; 2) PPIG4 dendrimers as carriers for *DJ-1* siRNA; 3) PEG, as an enhancer of nanoparticles stability and biocompatibility and 4) LHRH peptide, as a targeting moiety to the ovarian cancer cells. The approach for preparation of the nanoplatform consists of the following steps: 1) Complexation of negatively charged *DJ-1* siRNA by the positively charged PPIG4 into nanometer-sized complexes via electrostatic interactions; 2) Modification of the PPIG4-siRNA complexes with hydrophilic polymer by conjugation of PEG to PPIG4 amino groups on the nanoplatform surface; (3) Conjugation of LHRH peptide to the distal end of PEG layer through the maleimide (MAL) groups on the PEG and the thiol groups in LHRH peptide. Due to the electrostatic interactions, the positively-charged dendrimer and negatively-charged siRNA molecules spontaneously self-assemble into nanoparticles. An excess of dendrimers results in encapsulation of siRNA molecules inside of the nanoparticles and provides net positive charge on the nanoparticle surface, which in turn protect the siRNA against serum nuclease degradation and facilitate cellular internalization.

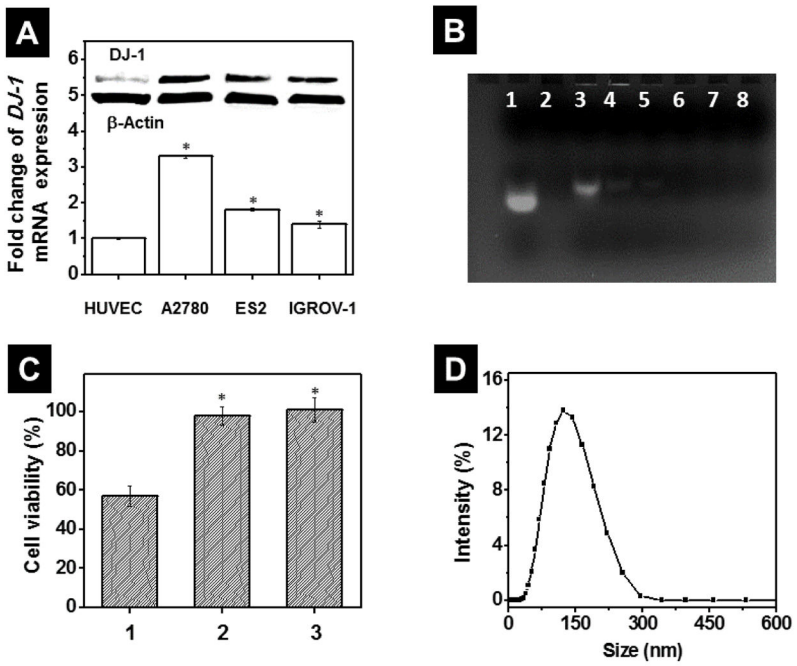

Figure 3.

(A) Basal level of *DJ-1* mRNA in non-malignant HUVEC and A2780/CDDP, ES2 and IGROV1 ovarian cancer cells measured by quantitative PCR. The intracellular level of DJ-1 in HUVEC cells was used as a reference and set to 100%. Means ± SD are shown. *$p < 0.05$ when compared with HUVEC cells. **Inset:** Representative Western blot images of DJ-1 protein and β-Actin expression in HUVEC, A2780/CDDP, ES2 cells and IGROV1 cells. **(B)** Representative agarose gel electrophoresis image of free siRNA (lane 1), PPIG4 (lane 2) and siRNA incubated with PPIG4 at the following N/P (PPIG4 amine: siRNA phosphate groups) ratios: 0.5 (lane 3), 1 (lane 4), 2 (lane 5), 4 (lane 6), 8 (lane 7) and 10 (lane 8). An efficient binding of siRNA molecules with PPIG4 retards their gel electrophoretic mobility and prevents siRNA staining by ethidium bromide (lanes 4–8) in comparison to free siRNA (lane 1). **(C)** Viability of A2780/CDDP cells after incubation for 48 h with (1) non-modified PPIG4-siRNA complexes loaded with scrambled siRNA (1μM), (2) PPIG4-siRNA complexes modified with PEG only and (3) PPIG4-siRNA complexes modified with both PEG and LHRH peptide (siRNA-NP). Means ± SD are shown. *$p < 0.05$ when compared with cancer cells treated with non-modified PPIG4-siRNA complexes. **(D)** Size distribution profile of siRNA-NP evaluated by dynamic light scattering.

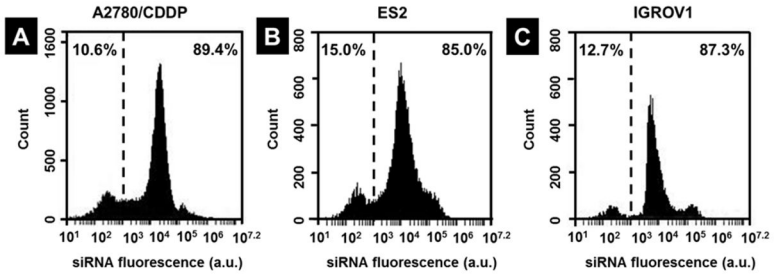

Figure 4.

Flow cytometry analysis validates high cellular internalization efficiency of LHRH-targeted nanoplatform loaded with DY-547-labeled siRNA after incubation with **(A)** A2780/CDDP, **(B)** ES2 and **(C)** IGROV1 ovarian cancer cells for 24 hours. The values on the right side of the dashed line indicate percentage of cell population transfected with the fluorescent siRNA.

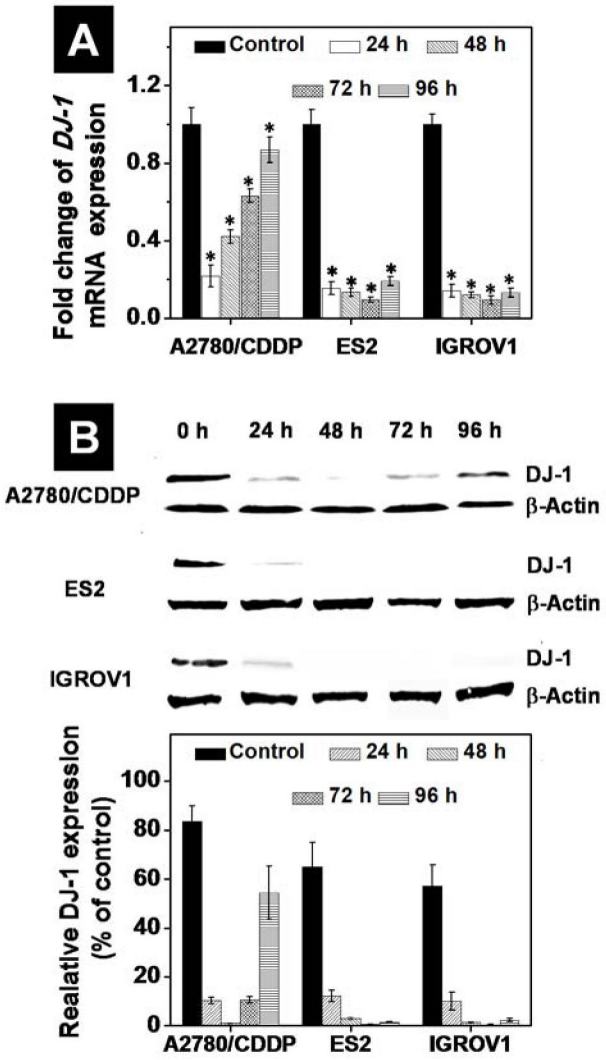

Figure 5.

Quantitative PCR analysis **(A)** and band densitometry analysis of Western blots **(B)** reveal expression of *DJ-1* mRNA and corresponding protein levels in A2780/CDDP, ES2 and IGROV1 ovarian cancer cells before (basal level) and after treatment with the *DJ-1* siRNA-loaded nanoplatform for 24 h. Band intensities of DJ-1 protein are expressed as the percentage of the β-actin band intensity, which was set as 100%. Time point evaluation (24–96 h) was performed to determine the duration of the siRNA silencing effect on DJ-1 levels following a single transfection in all cell lines. Means ± SD are shown. *$p < 0.05$ when compared with untreated cancer cells.

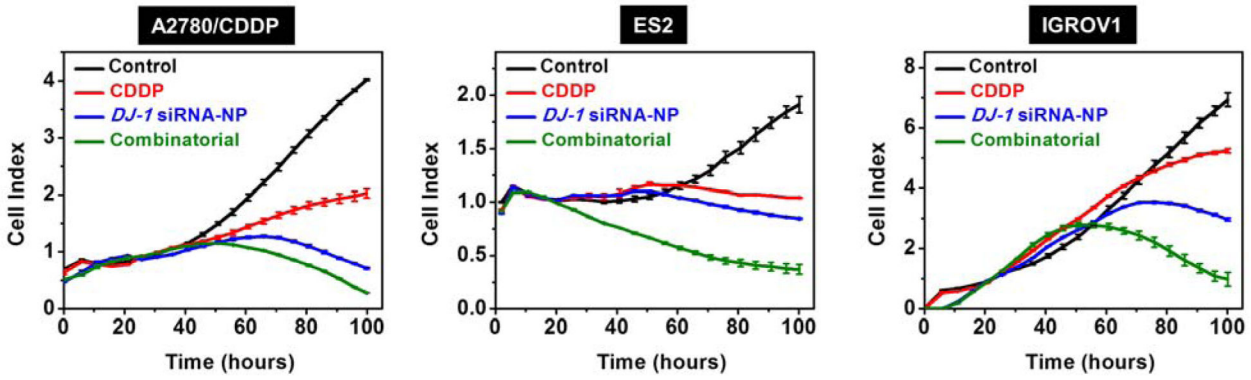

Figure 6.

Real time proliferation curves of A2780/CDDP, ES2 and IGROV1 ovarian cancer cells treated with media (control), CDDP, *DJ-1* siRNA-loaded nanoplatform and combinatorial therapy. The *DJ-1* siRNA-NP (siRNA = 1μM) and CDDP at the corresponding IC50 concentrations (A2780/CDDP = 23.6 μM, ES2 = 3.8 μM and IGROV1 = 1.9 μM) were added to the appropriate wells 2 h and 24 h, respectively after the cells were seeded in the E-plate. In case of the combinatorial therapy, the siRNA-NP and CDDP were consequently added to the assigned wells 2 h and 24 h, respectively after the cells were seeded in the E-plate.

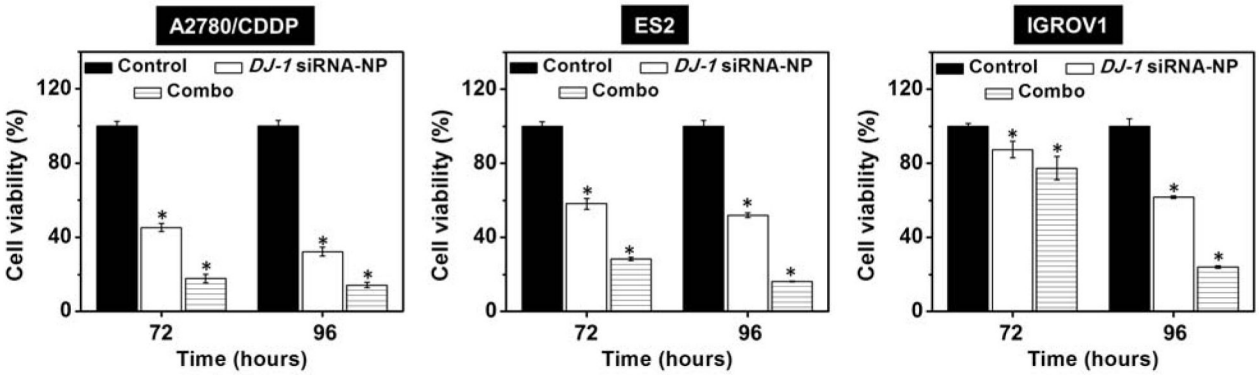

Figure 7.

Viability of A2780/CDDP, ES2 and IGROV1 ovarian cancer cells after treatment with media (control), *DJ-1* siRNA-loaded nanoplatform and combinatorial therapy (Combo). Means ± SD are shown. *$p < 0.05$ when compared with cancer cells treated with media.

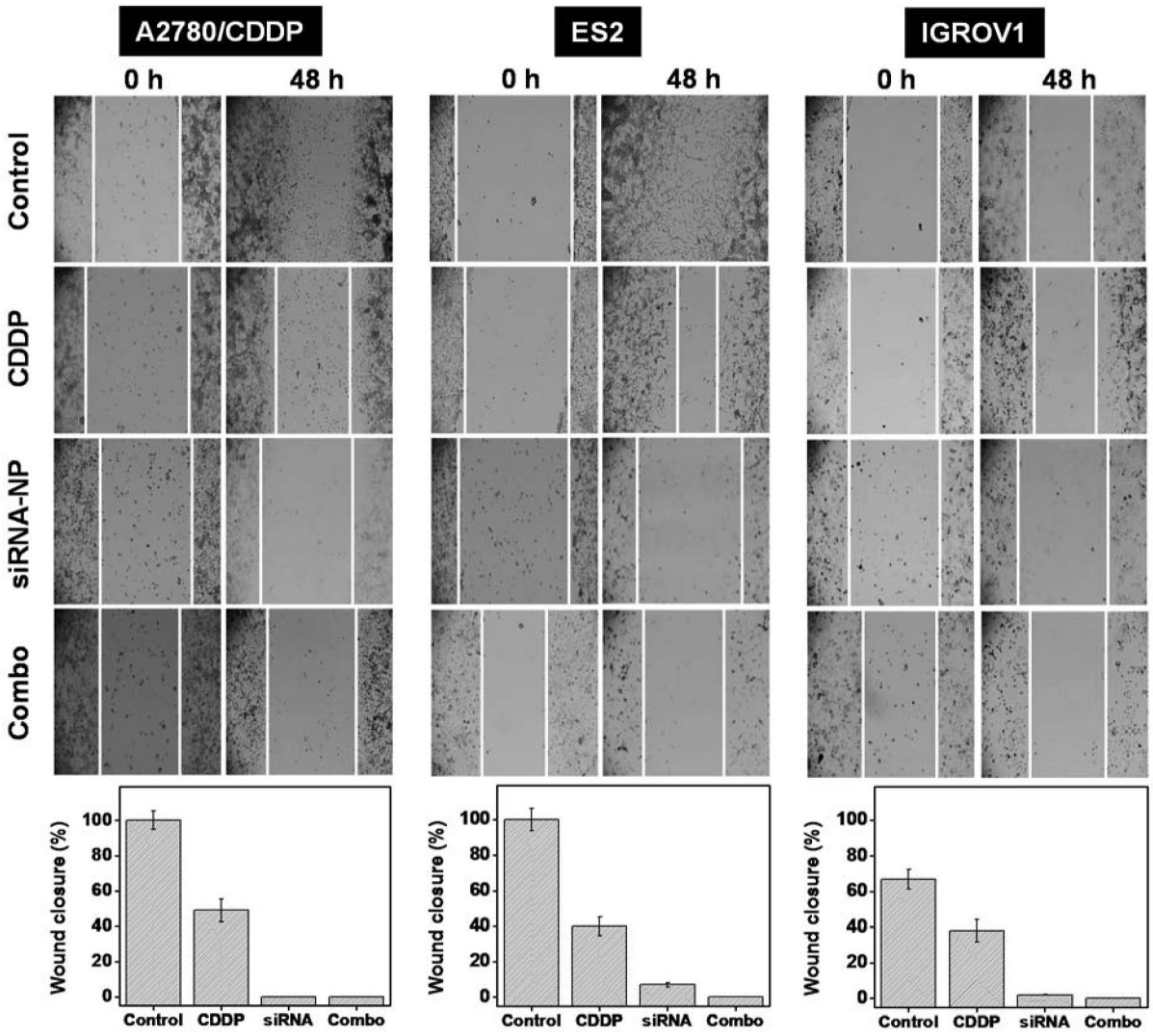

Figure 8.

A wound healing assay was employed to assess the migration of A2780/CDDP, ES2 and IGROV1 cells exposed to media (control), CDDP, *DJ-1* siRNA-NP and combinatorial therapy within 48 h. White lines represents cellular migration border.

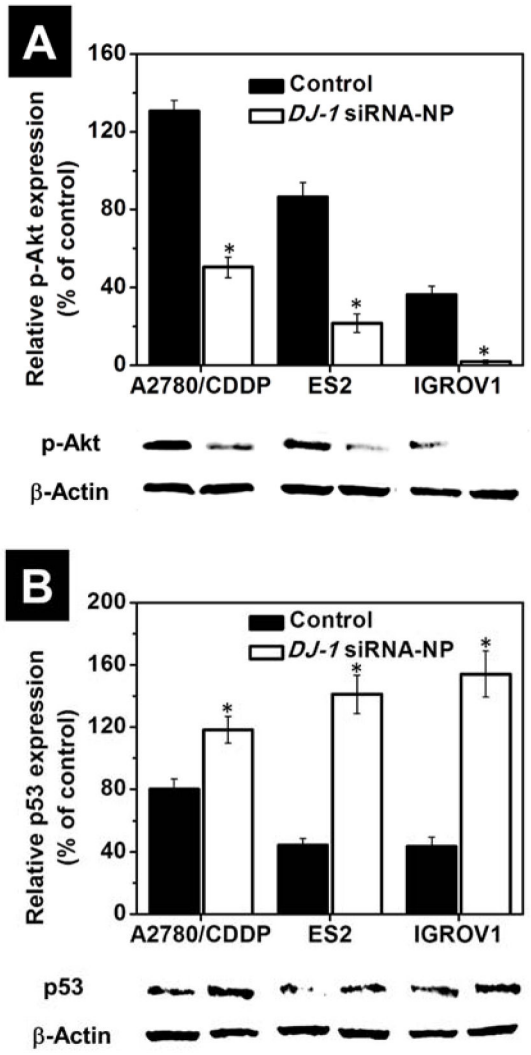

Figure 9.

The intracellular level of phosphorylated Akt **(A)** and p53 **(B)** proteins in A2780/CDDP, ES2 and IGROV1 cells before after treatment with *DJ-1* siRNA-NP for 24 h. Expression of proteins was evaluated by band densitometry analysis of Western blots from replicate experiments. Band intensities of phosphorylated Akt and p53 proteins are expressed as the percentage of the β-actin band intensity, which was set as 100%. Means ± SD are shown. *$p < 0.05$ when compared with cancer cells treated with media. Representative Western blot images of phosphorylated Akt, p53 and β-actin proteins expression in the ovarian cancer cells before and after exposure to the *DJ-1* siRNA treatment are provided.

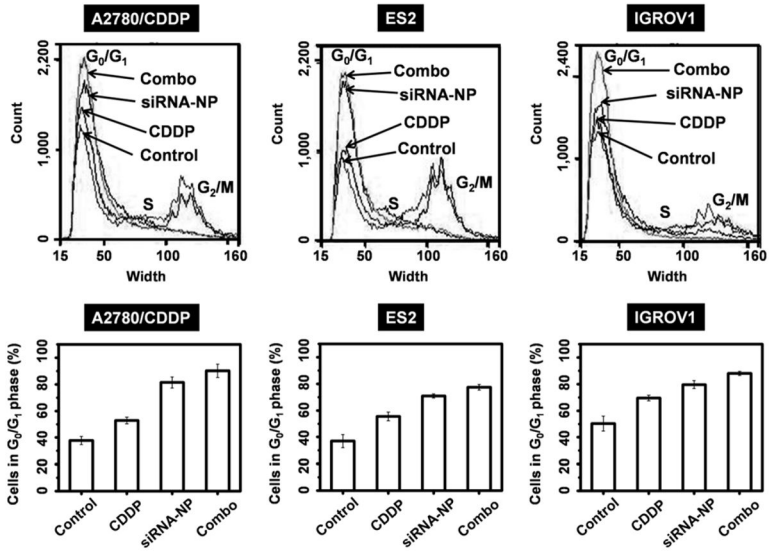

Figure 10.

Cell cycle alteration in A2780/CDDP, ES2 and IGROV1 ovarian cancer cells after treatment with CDDP, *DJ-1* siRNA-NP or combinatorial therapy. **Top panel** shows th**e** results of flow cytometry analysis using Vybrant® DyeCycle stain. **Bottom panel** depicts the percentage of A2780/CDDP, ES2 and IGROV1 cells in G_0/G_1 phase of the *cell cycle* before and after treatment with CDDP, *DJ-1* siRNA-NP and combinatorial therapy.

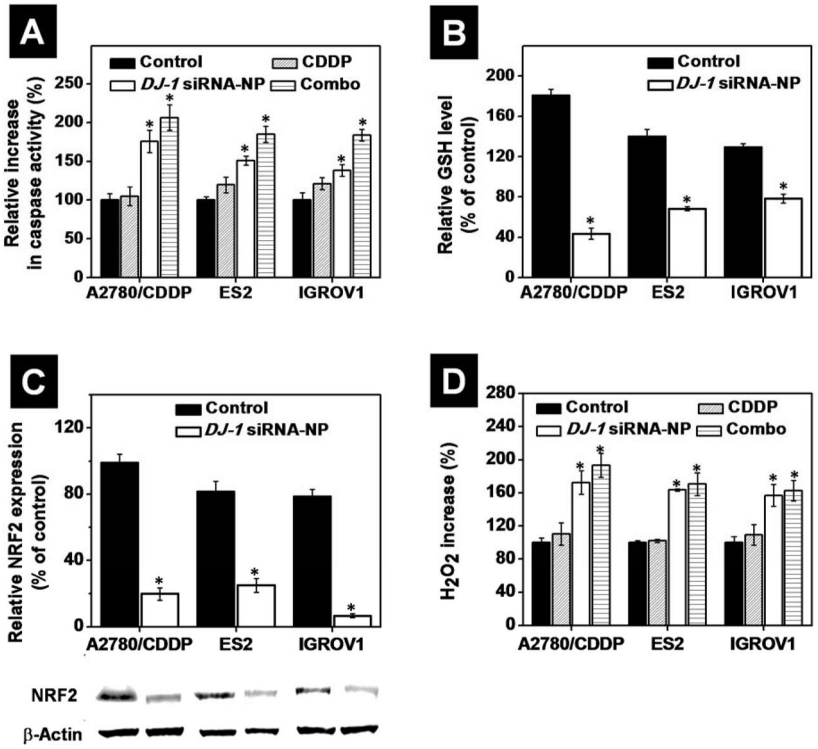

Figure 11.

(**A)** The relative increase in caspase-3/7 activity in A2780/CDDP, ES2 and IGROV1 cells before after treatment with CDDP, *DJ-1* siRNA-NP and combinatorial therapy. The caspase activity was set to 100%. **(B)** The relative intracellular level of reduced glutathione (GSH) in ovarian cancer (A2780/CDDP, ES2 and IGROV1) cells before and after treatment with *DJ-1* siRNA-NP for 24 h. The intracellular level of GSH in non-treated HEK293 cells was used as a reference and set to 100%. (**C)** The intracellular level of NRF2 protein in A2780/CDDP, ES2 and IGROV1 cells before after treatment with *DJ-1* siRNA-NP for 24 h. Expression of proteins was evaluated by band densitometry analysis of Western blots. Band intensities of NRF2 protein in the various samples are expressed as the percentage of the β-actin band intensity, which was set to 100%. Representative Western blot images of NRF2 proteins expression in the ovarian cancer cells before and after exposure to the *DJ-1* siRNA treatment are provided. (**D)** Relative intracellular level of H_2O_2 in the ovarian cancer cells after treatment with CDDP, *DJ-1* siRNA-NP and combinatorial therapy. Cells incubated with media were used as the control and intracellular level of H_2O_2 in these cells was set to 100%. Means ± SD are shown. $*p < 0.05$ when compared with cancer cells treated with media.